PROCEEDINGS OF SPIE

SPIEDigitalLibrary.org/conference-proceedings-of-spie

Using the Spitzer IRAC science archive for instrument trending

Jessica Krick, Jim Ingalls, Patrick Lowrance, Sean Carey, Jessie Christiansen, et al.

Jessica Krick, Jim Ingalls, Patrick Lowrance, Sean Carey, Jessie Christiansen, William Glaccum, Carl Grillmair, Seppo Laine, "Using the Spitzer IRAC science archive for instrument trending," Proc. SPIE 10698, Space Telescopes and Instrumentation 2018: Optical, Infrared, and Millimeter Wave, 106985Y (6 July 2018); doi: 10.1117/12.2310185

Event: SPIE Astronomical Telescopes + Instrumentation, 2018, Austin, Texas, United States

Downloaded From: https://www.spiedigitallibrary.org/conference-proceedings-of-spie on 2/8/2019 Terms of Use: https://www.spiedigitallibrary.org/terms-of-use

Using The Spitzer IRAC Science Archive for Instrument Trending

Jessica Krick[a], James Ingalls[a], Patrick Lowrance[a], Sean Carey[a], Jessie Christiansen[a], William Glaccum[a], Carl Grillmair[a], and Seppo Laine[a]

[a]IPAC/Caltech, 1200E. California Blvd, Pasadena, USA

ABSTRACT

We present a database of reduced data for all staring mode observations taken with the Infrared Array Camera (IRAC) during the *Spitzer* warm mission to monitor instrument performance, predict future instrument performance, and facilitate exoplanet and brown dwarf science. Our motivation is to be informed so that we can mitigate the impact of changing thermal conditions on science. Monitoring current trends allows us to predict future instrument performance and to adjust our recommended suite of best practices and calibrations accordingly. From this database we show that instrumental effects detrimental to high precision photometry either remain stable or improve. A uniform reduction of all IRAC light curves has never before been published, and will enable powerful science including accurate comparative studies of exoplanets and brown dwarfs. IRAC has been performing well throughout the warm mission and we expect performance to remain excellent.

Keywords: Spitzer IRAC; trending; high precision photmetry; big data

1. INTRODUCTION

NASA's *Spitzer* Space Telescope[1] is on an earth-trailing orbit, moving further away from earth over time, currently at ∼1.6AU. As the distance from the Earth increases, the pitch angle of the spacecraft, defined as the angle between normal to the solar array and the Sun direction, must increase for communication. This illuminates the telescope in different ways, changes battery heating cycles, and has related secondary thermal effects. We continue to monitor changing thermal conditions for their impact on science quality as the mission extends to 2019 or beyond.

Standard data quality analysis consists of post facto checking for failed data, strange data features, etc. In particular, *Spitzer* maintains a calibration trending website including calibration, bias, and bad pixel measurements.[2] We improve on this practice by using a self-built database of exoplanet observations to monitor current trends over the roughly nine years since the warm mission began. The goal of the monitoring is to specifically look for changes in correlated noise which affect high precision photometry data, and so we use the high precision photometry data itself from the archive to do this monitoring. Changes in the noise patterns can be caused by variations in movements of the star across the pixel. These correlated noise patterns must be tracked because they can mimic the astrophysical signal under study. We monitor areas such as drift in position as a function of time, or ability of the telescope to re-point to the "sweet spot" accurately. We have defined the"Sweet Spot" region of each array to be the 0.5-pixel square surrounding the point of maximum response in the Subarray Field-of-View center pixel (pixel [15,15] in [0,0]-based coordinates). Specifically the sweet spot peak is at [15.198, 15.020] in ch1 and [15.120, 15.085] in ch2. The "sweet spot" was chosen to be the region of lowest gain variation thereby minimizing correlated noise. Keeping track of patterns in these metrics allows us to predict future instrument performance and to adjust our suite of suggested best practices for observation planning, calibrations, and data reduction.

One of the great legacies of the *Spitzer* Infrared Array Camera (IRAC)[3] instrument will be its contribution to the field of extrasolar planets. Throughout the warm mission, exoplanets have routinely accounted for 25% of allocated *Spitzer* time. This constitutes just over two years of valuable observing time allocated to the study

Further author information: (Send correspondence to J.K.)
J.K.: E-mail: jkrick@caltech.edu, Telephone: 1 6263951975

Space Telescopes and Instrumentation 2018: Optical, Infrared, and Millimeter Wave, edited by Makenzie Lystrup, Howard A. MacEwen, Giovanni G. Fazio, Proc. of SPIE Vol. 10698, 106985Y
© 2018 SPIE · CCC code: 0277-786X/18/$18
· doi: 10.1117/12.2310185

Downloaded From: https://www.spiedigitallibrary.org/conference-proceedings-of-spie on 2/8/2019
Terms of Use: https://www.spiedigitallibrary.org/terms-of-use

of exoplanets. The publicly available IRAC data archive is incredibly rich, including roughly 1500 exoplanet observations in either transit, eclipse, or over full phase curves. However, the majority of these observations have not been published, and those that are already in the literature have typically been studied as individual sources using data reduction techniques tailored to each observation. Despite this existing archive, the community has, until now, been unable to perform a large comparative study of the properties of the exoplanets and brown dwarfs observed by *Spitzer* in a way that is free from the uncertainties introduced by different reduction techniques. The database generated for this monitoring project is the so far missing piece in the puzzle of putting together comparative exoplanet studies.

2. DATA AND PHOTOMETRY CATALOG

Making a uniform database from a non-uniform dataset is challenging. A non-exhaustive list of categories in which each IRAC observation differs from others include: total duration, exposure time, channel, use of peak-up on the target star, guide star, or not at all, pitch angle of the telescope during the observation, pitch angle of the telescope during the previous observation, sub-pixel region where the target star landed, observation labeling by the observer (i.e., the target name), whether a suggested 30 minute pre-observation was taken, and whether it was dithered or employed staring mode. Observations can be taken in one or both channels, commonly referred to as channel 1 at 3.6 μm and 4.5 μm. Some observations will simply not be included in our database because they are unidentifiable for any of the above reasons. However, for overall telescope trending, it is sufficient to use a large representative sample.

2.1 Building the Database

To achieve the goal of capturing the majority of the high precision photometry observation in the archive for our database we start by gathering all observations which are long in duration and that have a certain set of program IDs which the *Spitzer* Science Center (SSC) identifies as being exoplanets or brown dwarfs. The archive does not actually track whether an observation is staring or dithering, which would be the definitive factor, so we use duration and ID as a proxy. As of the writing of this paper, the archive includes $\sim$ 1200 observations between 2.0 and 10.5 hours, and $\sim$ 500 observations longer than 10.5 hours. Sequential observations of the same target are then linked, and we also track the previous observation, regardless of target, so that we can measure telescope properties before the high precision photometry observations begin. We measure the pitch angle of the telescope both during the target observation and during the previous observation to measure what the change in pitch was between observations.

One issue in reproducing exoplanet photometry is identifying which target in the field of view is the exoplanet being observed. Observers are not required to include this information when designing observations, and especially early in the mission, targets were placed all over the detector, not just on the "sweet spot" pixel recommended for exoplanet observations. We have written an automated code to determine the likely target by searching public exoplanet archives near the position of the field of view. The algorithm first performs an automated API search of NExScI followed by Simbad. Then, if it still hasn't found a candidate, the algorithm will choose the brightest peak in the image which is not within ten pixels of the edge of the frame.

After the target has been identified, we perform center-of-light centroiding, aperture photometry, background calculation in an annulus outside the source, noise pixel calculation (a measure of the point spread function apparent size),[4] and we store pixel values around the target center. Finally, from all extracted light curves we measure long and short-term drifts in position. Long-term drift is a nearly linear drift in the measured position of a star during an observation and is of order 0.3 arcsec/day in the Y direction.[5] Short-term drifts in position are usually of order 0.1 arcesconds in amplitude and have durations less than two hours at the beginning of an observation. Not all observations show short or long-term drifts. These drifts are discussed further in section 3.1 and 3.3.

Only two steps in this process are not completely automated. Firstly, the SSC manually maintains a list of exoplanet program IDs which we use for deciding which observations to include in the database. Secondly, we manually indicate on a plot of centroids as a function of time where the short-term drift starts and finishes; at this point the code calculates a duration and slope of the drift. To date, our database has over 70 million records (each aperture photometry measurement during each observation), and includes 49 attributes (columns).

Downloaded From: https://www.spiedigitallibrary.org/conference-proceedings-of-spie on 2/8/2019
Terms of Use: https://www.spiedigitallibrary.org/terms-of-use

2.2 Removing Correlated Noise

The main systematic in high precision photometry with IRAC is intrapixel gain variations. We see variations in measured flux due to the combination of under-sampling the point spread function (PSF) and small motions of the telescope, which move the light around within a single pixel. Since over 40% of the light in the PSF falls in that single pixel, the total light curve can vary by up to eight percent in channel 1 at 3.6 μm and a few percent less in channel 2 at 4.5 μm. This is of order 10 to 100 times the astrophysical signal under investigation.[6] We see sensitivity variations across the pixel on scales as small as 0.005 pixels. Since some motion of the telescope is unavoidable, researchers have developed non-linear analysis methods to mitigate these correlated signals.[6–14]

The database currently includes an initial pixel-level de-correlation (PLD) systematics reduction,[11] one of the most commonly used systematics reductions in the literature. This is 'first-look' only since PLD relies on simultaneously fitting the astrophysical signal with the noise model, which requires simultaneous de-coupling of noise and astrophysical signal and requires human intervention. Our goal is development of an entirely automated data reduction method which uses the calibration data, and not the observations themselves, to remove correlated noise from the light curves. Currently in development is a very promising machine learning technique using random forests to determine the intrapixel gain function from calibration data.

3. TELESCOPE PERFORMANCE

Because telescope motions are so critical to the main systematic in IRAC high precision photometry, we focus our efforts mainly on monitoring telescope motions as a function of time. To look for changes in telescope motions, we monitor the following quantities: long-term drift, cloud size, short-term drift, and position oscillations. To look for changes in pointing, we monitor average positions on the array. Automatically generated trending plots based on the database are displayed on an internal website for instrument scientists to monitor on a monthly basis. These plots are scatter plots and violin plots to allow instrument scientists to visually draw conclusions about trends. With our rich database of hundreds of observations, violin plots allow us to show smoothed distributions in bins along with their median values and inner quartile range. Violin plots are color-coded by year to distinguish each year, but color does not carry any other significance.

Aside from the specific quantities listed above, which we monitor on a monthly basis, we are also able to monitor topics as they arise. These can be either anomalous behavior noted by the instrument teams, or queries that arise from users. We have in the past gotten questions from users through the *Spitzer* Helpdesk as to whether or not their particular observations are anomalous or "what went wrong?". We are able to use the monitoring database to statistically show the answer to some of those questions, i.e., how often do certain data features occur?, are they true outliers or tails of the distributions?, and if a certain observation did not land on the sweet spot, was that a specific problem with an observation, or something systemic.

3.1 Long-term Drift

Long-term drift is measured as smooth changes in position of the target star over the entire duration of the observation, and is of order a few tenths of a pixel per day. Because short-term drift often dominates the first half hour of any given observation, we measure long-term drift as the change in position from 30 min. after the beginning of the observation till the end of the observation. Long and short-term drifts have different causes and so are discussed here in separate sections. Long-term drift is caused by the way that differential velocity aberration corrections are handled by the spacecraft's Command and Data Handling computer (C&DH) and by the star trackers. We monitor rate of long-term drift because changes in position are the largest cause of noise in exoplanet light curves. Figure 1 shows the automatically measured drift in both X and Y position (top and bottom panels respectively) as a function of time on the left side and pitch to earthpoint on the right side. Earthpoint is the pitch angle required to downlink data to the Earth. Pitch to earthpoint changes throughout the mission as *Spitzer* moves further away from Earth and around the Sun in it's Earth-trailing orbit. Note: Pitch to earthpoint is different from the pitch angle of any given observation as discussed in Section 3.3.

We are currently monitoring a slight increase in the long-term drift in the X direction, which so far is noticeable but does not significantly affect science. Median drift rate values in 2017 and 2018 are -0.005 pixels per hour, which is an apparent increase over the median values of -0.002 pixels per hour before 2017. Because

Downloaded From: https://www.spiedigitallibrary.org/conference-proceedings-of-spie on 2/8/2019
Terms of Use: https://www.spiedigitallibrary.org/terms-of-use

pitch to earthpoint and time are correlated, it is hard to disentangle trends seen in these plots. However, since pitch to earthpoint is a more physical variable describing a change in the telescope, as opposed to time, we think this is the likely true correlation. We already have mitigation strategies in place for drifts in the Y direction which are still larger than those in X direction, and those strategies will also take care of the increased X drift. Mitigation strategies include re-peaking up on the target star every 12 hours during a long observation, and designing data reduction techniques which can accommodate slight drift. We assume that this extra X drift is responsible for the cloud size increase in the X direction noted below.

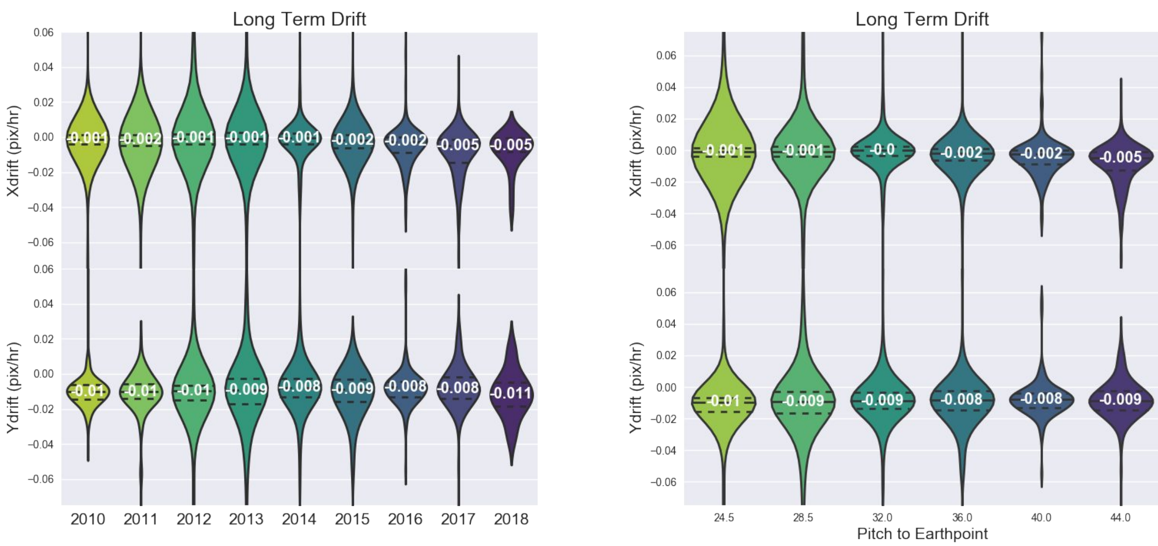

Figure 1. **Distribution of Long-term drift in both the X and Y directions as a function time on the left and of nearest in time downlink pitch angle on the right**. Left: Long-term Y drift remains constant over the 8.5 years of the entire warm mission. X drift appears to have increased over the past two years. Right: This plot is for 2012 onward only, so doesn't include the first two years of the warm mission. We see the same trends as in the long-term drift with time plots. Potentially the physical variable which is increasing the X drift over time is the increased downlink pitch angles, but it is not possible to de-correlate this from time since pitch angles are increasing over time.

3.2 Cloud Size

One diagnostic of the motions of the telescope within a long staring observation is the size of a cloud of the measured centroids. Many observations have hundreds or thousands of individual images and therefore the same number of centroids. As some motions of the telescope are unavoidable, all observations will necessarily have centroids during the observation which fill in a "cloud" in X-Y position space. We measure the standard deviation of the cloud of positions in both the X and Y directions to monitor telescope motions. Small cloud sizes, or smaller total motion, is ideal for high precision photometry since motions move the center of light around on the pixel, which is associated with intrapixel gain variation. The left side of Figure 2 shows a scatter plot of all cloud sizes in gray and only those from the last six months in red. The right side of Figure 2 is a violin plot showing the distributions of X (top) and Y (bottom) standard deviations per year over the nine years of the warm mission. We find a slight increase in the X motions of the telescope beginning in 2017 continuing into the limited data available in early 2018. This is most evident in the scatter plot, but also in the violin plots. The Y distribution hints at a change, but is currently not a three sigma change. We continue to monitor this but note that mitigation strategies already in place are more than enough to accommodate the extra X motions.

Downloaded From: https://www.spiedigitallibrary.org/conference-proceedings-of-spie on 2/8/2019
Terms of Use: https://www.spiedigitallibrary.org/terms-of-use

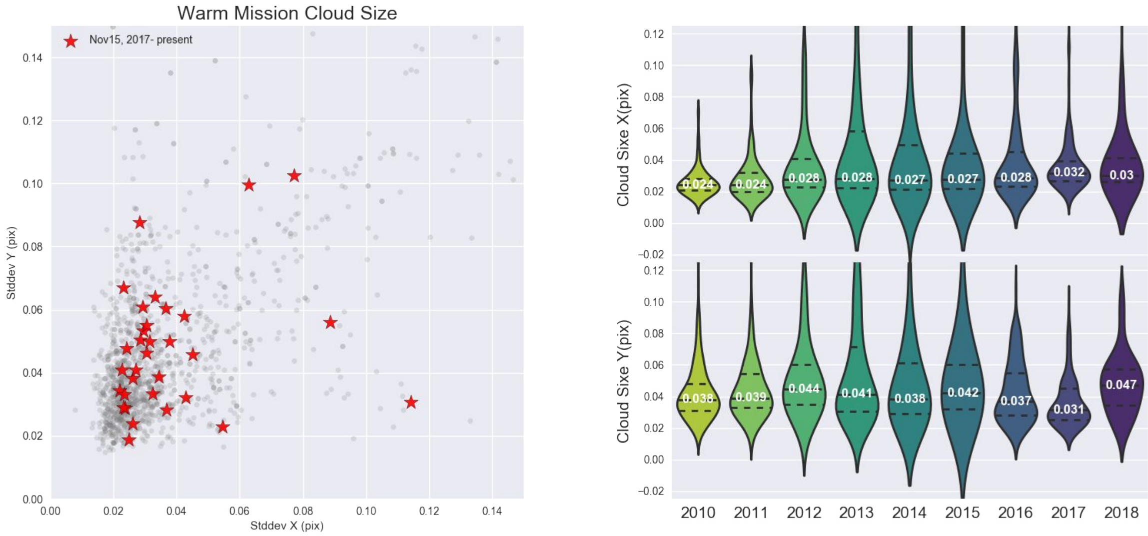

Figure 2. **Standard deviations in position in both the X and Y directions as a scatter plot on the left and a function time on the right** Left: gray points show all warm mission cloud sizes; red points show the last six months. Right: distributions of standard deviations have been binned and smoothed on year timescales over the warm mission. Medians and inner quartile ranges are indicated with their numeric values and dashed lines, respectively.

3.3 Short-term Drift

Short-term drift is the slow change in position over the first roughly half hour to two hours of a non-dithered observation. We measure this by having the code display the full light curve of position as a function of time for both the recommended pre-observation and the science observation, and manually marking the start and end of the drift. Figure 3 shows only Y centroid drifts as the drift appears to be limited to the Y direction. We monitor short-term drift for the purpose of tracking all telescope motions. Figure 3 shows the Y centroid short-term drift as a function of pitch angle of the observation itself on the left and on the right as a function of change in pitch angle from the previous observation. Each plot has three panels: the top shows the duration of the short-term drift ranging from no drift to 2.4 hours with a median of around 0.5 hours. The middle panel is the total length of the drift in pixels, and the bottom panel shows the slope of the drift in pixels per hour. Points are color-coded by exposure time for which we see no evidence of a correlation.

We do see evidence that both the scale and rate of the short-term drift are correlated with pitch angle of the observation and more strongly correlated with the change in pitch angle from the previous observation. This leads us to the conclusion that short-term drift is caused by a thermal settling of the telescope as it gets different illumination from the Sun through different pitch angles relative to the Sun, an idea first put forth in reference 5. These correlations are likely not perfect because a) it is hard to measure the exact start and finish time of a drift superimposed on top of the other changes in position of the centroids discussed in this paper, and b) there is likely a correlation also with even earlier observations. The scale and rate of the short-term drift probably depends on the pitch angle and duration of several previous observations.

3.4 Position Oscillations

Early warm mission observations showed distinct oscillations in position that looked like a sawtooth pattern in position as a function of time. These oscillations were of order 60 minutes at the beginning of the warm mission and are due to battery heater cycling with a period of roughly 60 minutes. At the end of 2010, the battery heater temperature excursions were changed from one degree Celsius to half a degree Celsius. This reduced the period of the oscillations to roughly 40 minutes. This change was initiated by the desire to remove the 60

Downloaded From: https://www.spiedigitallibrary.org/conference-proceedings-of-spie on 2/8/2019
Terms of Use: https://www.spiedigitallibrary.org/terms-of-use

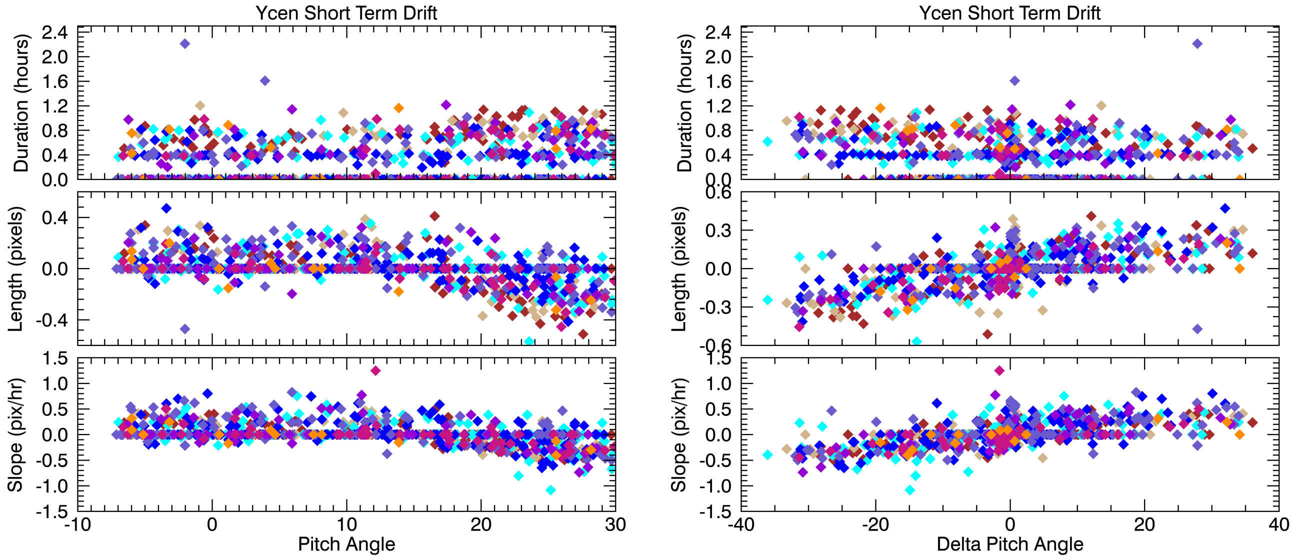

Figure 3. **Short-term Drift** Left: duration, length and slope of the short-term drift as a function of pitch angle of the observation itself. Right: same short-term drift parameters as a function of change in pitch angle from the previous to the current observation. Observations are color coded by exposure time where shorter exposures are red and longer exposures are blue.

minute oscillations from exoplanet light curves since that is a similar timescale to astrophysical events under investigation such as transit and eclipse durations.

Plots in figure 4 stem from a Lomb-Scargle periodogram of all positions in the observations. The bottom panel shows the period of the largest peak in the periodogram between 20 - 80 minutes, and the top panel shows the strength of that peak. We only search the 20-80 minute timeframe since periodograms will find peaks also at the total duration of observations, so we don't want that to be a source of confusion. Strength is measured relative to the other peaks detected. Dashed lines show the median and inner quartile values. We note the intentional change in 2010 of the peak period, followed by a flat period until 2014 when we note a slow increase in peak period over the rest of the warm mission. Simultaneously, the peak strength of the periodogram after 2014 goes toward zero. Zero peak strength indicates that the periodogram algorithm is no longer finding an oscillating pattern in the positions, and is instead measuring noise.

Since 2014, the spacecraft has been using the battery more during downlinks due to the increasing pitch angles that have lower solar irradiance of the solar panels. This battery usage then requires re-charging the battery during science observations and calibrations. This discharging and re-charging of the battery results in a higher operating temperature of the battery, therefore the battery heater comes on less frequently and often is not operating during science observations. Therefore, the pointing oscillations have, over time, disappeared from many, if not most, high precision staring mode observations. This is an improvement for scientists using IRAC for high precision photometry.

3.5 Average Position on the Array

The mean position on the array of an entire long observation is a diagnostic of being able to repeatably re-point the telescope to the "sweet spot". Pointing to the sweet spot is critical for high precision photometry because a) it is the region of least gain variation as a function of position and b) it is the only region of the pixel which has been calibrated by the *Spitzer* Science Center to characterize intrapixel gain variations. The edges of the pixel have a steeper gain change as a function of position, so targets landing there will have larger systematics introduced into light curves for the same amount of telescope movement compared to the center of the sweet

Downloaded From: https://www.spiedigitallibrary.org/conference-proceedings-of-spie on 2/8/2019
Terms of Use: https://www.spiedigitallibrary.org/terms-of-use

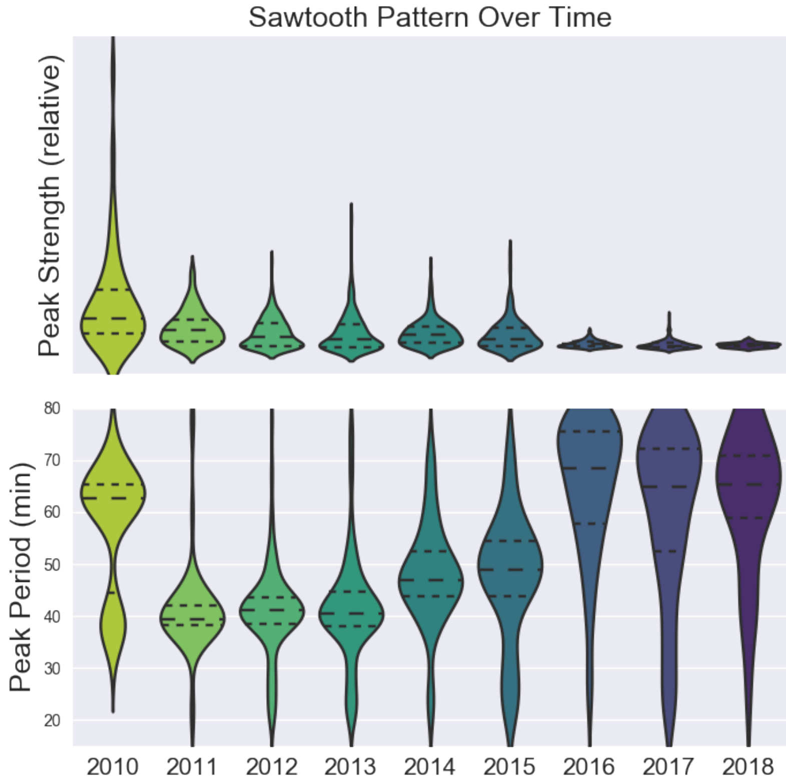

Figure 4. **Position oscillations throughout the warm mission** These plots show the results of periodogram calcuations on position as a function of time for each observation. The top panel shows the strength of the main peak in the periodogram relative to all other peaks as an indication of the amplitude of the oscillations. The bottom panel shows the distributions of the periods of the peak oscillations.

spot (near the center of the pixel). Figure 5 shows the entire warm mission mean positions in gray and those from the last six months in red. The right side of the figure shows a violin plot of distance from the sweet spot per year for only those observations that landed within one pixel of the sweet spot. At the observers' discretion, some observations do not use the sweet spot. Thus far we do not monitor if observations are using peak-up on the target star or on a guide star. If they are using a guide star, then astrometry errors of the target star will dominate pointing errors in determining the final position on the array. We intend to add the source of the peak-up to our database in the future, and continue monitoring these plots.

Just in the past few months we see a slight change in the average Y positions of observations. 2018 has so far only 24 observations near the sweet spot, and manually looking at those observations, most use guide-star peak up, so it is too early to draw conclusions about any trends, but we will continue to monitor these position plots.

4. ENABLING SCIENCE

In addition to monitoring telescope performance, the database provides a unique opportunity for exoplanet and brown dwarf researchers. The last two decades have seen a huge leap in our understanding of exoplanet atmospheres. From detections of individual atoms and molecules (from the original detection of sodium in the atmosphere of HD 209458b[15] to the recent announcement of helium in the atmosphere of WASP-107b[16]), to mapping out atmospheric structures both in depth (e.g. the detection of the thermal inversion in the atmosphere

Downloaded From: https://www.spiedigitallibrary.org/conference-proceedings-of-spie on 2/8/2019
Terms of Use: https://www.spiedigitallibrary.org/terms-of-use

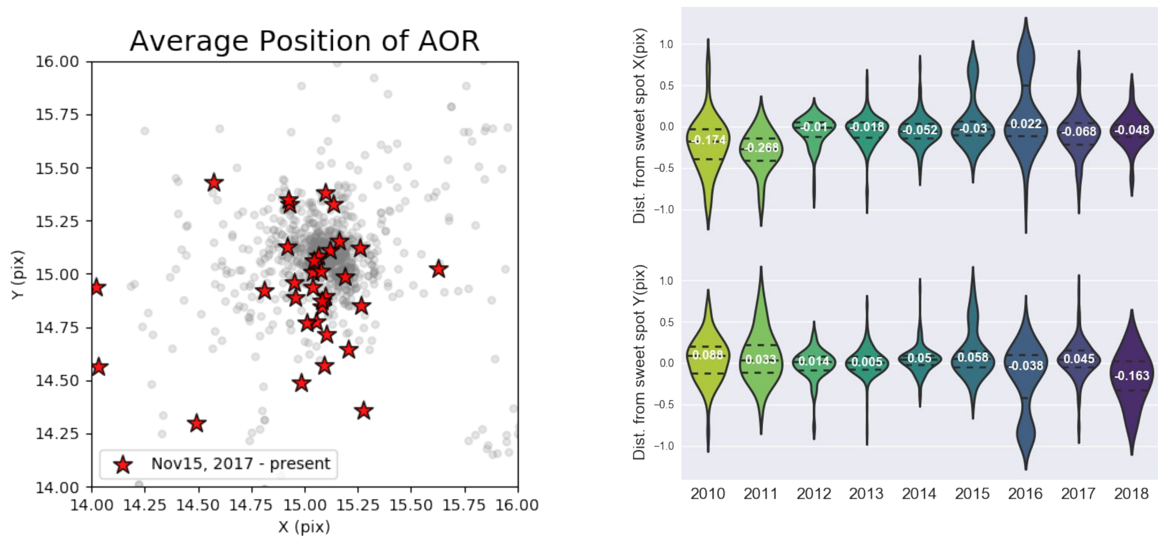

Figure 5. **Average Position on the Array** Left: One gray circle for the average position of the cloud of centroids for each observation. Red stars show the last six months of data. Right: distributions of distance from the sweet spot as a function of time throughout the warm mission. Top panel shows the X direction, and bottom panel shows the Y direction.

of HAT-P-7b[17]) and with longitude (e.g. the first longitudinal map of HD 189733b[18]), to identifying clouds (e.g. in the atmosphere of the super-Earth GJ 1214b[19]) and hazes (e.g., in the atmosphere of WASP-12b[20]) in upper atmospheres, we have continued to push our ability to glean new conclusions. One area that has many unresolved questions is the large-scale understanding of the observed differences among exoplanet atmospheres. Why do some exoplanet atmospheres show thermal inversions in their stratospheres while others do not? Why do some exoplanet atmospheres appear clear, while others appear cloudy? Which properties of the exoplanet host stars manifest themselves in the observed properties of the exoplanet atmosphere, and how? Potential science goals using this archive are to allow both a comprehensive, comparative exoplanet analysis and comparative brown dwarf analysis, and to increase the diversity of exoplanet researchers working in the field.

A uniform reduction of publicly available IRAC data is the most comprehensive, robust approach to performing a comparative exoplanet atmosphere study. With these archived data, researchers will have the unique ability to perform a very large-scale, uniform analysis of the atmospheric properties of exoplanet populations. Three potential exoplanet science goals for the database include:

- examining the relative strengths of the 3.6-μm and 4.5-μm eclipse depths as a function of planet mass to study planet formation theories linking planet mass and atmospheric metal content;
- searching for a discriminator between clear and cloudy hot Jupiter atmospheres to aid target selection for future observations with NASA facilities; and
- studying the day-night contrast and super-rotational winds as a function of planet and stellar properties by looking at the ensemble of phase curves or potentially stacking phase curves of exoplanets with similar property.

Brown dwarf science with the IRAC instrument broadly includes monitoring light curve evolution on minute- to day-long timescales to analyze atmospheric changes and cloud formation.[21–23] For example, Jupiter exhibits variability on many different scales from minutes to centuries. Certain convective events have been observed on minute timescales, cloud vortices can form and merge on days to weeks, while the Great Red Spot has been fairly stable with small significant morphology changes over decades. Understanding the physics and evolution

Downloaded From: https://www.spiedigitallibrary.org/conference-proceedings-of-spie on 2/8/2019
Terms of Use: https://www.spiedigitallibrary.org/terms-of-use

of condensate clouds across the temperature scale from 600K to 1800K is important to correctly interpret atmospheric signatures in giant exoplanets in close orbits to their stars. With homogeneously reduced light curves across multiple epochs and spectral types, correlations of variability across temperature, rotation period, and mass/age can lead to further understanding of atmospheric dynamics of the cloud covers in brown dwarfs.

Perhaps the most important outcome of this monitoring database is that it opens the field of exoplanets and brown dwarfs to astronomers who are not experts with the IRAC detector or the myriad available data reduction techniques. By lowering the barrier to entry with an already compiled, cleaned, homogeneous data-set, our project is intended to improve the inclusion and diversity of scientists working on IRAC exoplanets. Providing full access to quality data to a variety of researchers will promote the diversity of researchers in the field, thereby bringing new perspectives, and improving the science output.[24]

5. CONCLUSIONS

We monitor telescope motions and pointing by using a uniform reduction of the IRAC science archive. The uniform database has been carefully built by overcoming challenges in non-uniformity amongst all archival observations. Telescope motions are monitored through automatically generated plots of long-term drift, cloud size, short-term drift, and position oscillations. Pointing is monitored through tracking the average positions on the array. We conclude from our monitoring that the *Spitzer* telescope is performing at or beyond 2010 standards and we expect that to continue. While we do note slight changes in telescope performance, none are significant to science performance, so we expect excellent science to continue in the warm mission. In the era of big data tools being relatively easy to learn, we have described a practical way of using free science archival data to both fully understand systematics of the instrument, and to look for trends which help to predict the future.

In particular, the uniform database itself enables exoplanet and brown dwarf science. Examples of that science include studying the atmospheres and thermal properties across the full range of size and temperatures represented by both exoplanets and brown dwarfs. The ultimate goal of this type of science is informing planet formation models.

For future missions, we encourage attempts at uniformity in data and documentation in everything from how the data are taken to how the data are stored, naming conventions, special observations, and maintaining archives. This benefits not only science but attempts at trending performance.

REFERENCES

[1] Werner, M. W., Roellig, T. L., Low, F. J., Rieke, G. H., Rieke, M., Hoffmann, W. F., Young, E., Houck, J. R., Brandl, B., Fazio, G. G., Hora, J. L., Gehrz, R. D., Helou, G., Soifer, B. T., Stauffer, J., Keene, J., Eisenhardt, P., Gallagher, D., Gautier, T. N., Irace, W., Lawrence, C. R., Simmons, L., Van Cleve, J. E., Jura, M., Wright, E. L., and Cruikshank, D. P., "The Spitzer Space Telescope Mission," *ApJS* **154**, 1–9 (Sept. 2004).

[2] Lowrance, P. J., Krick, J., Ingalls, J., Laine, S., Carey, S., Glaccum, W., Hora, J., and C., G., "Calibration Trending in the Spitzer Beyond Era," in [*Space Telescopes and Instrumentation 2018: Optical, Infrared, and Millimeter Wave*], *Proceedings of the SPIEE* **1**, 1 (Aug. 2018).

[3] Fazio, G. G., Hora, J. L., Allen, L. E., Ashby, M. L. N., Barmby, P., Deutsch, L. K., Huang, J.-S., Kleiner, S., Marengo, M., Megeath, S. T., Melnick, G. J., Pahre, M. A., Patten, B. M., Polizotti, J., Smith, H. A., Taylor, R. S., Wang, Z., Willner, S. P., Hoffmann, W. F., Pipher, J. L., Forrest, W. J., McMurty, C. W., McCreight, C. R., McKelvey, M. E., McMurray, R. E., Koch, D. G., Moseley, S. H., Arendt, R. G., Mentzell, J. E., Marx, C. T., Losch, P., Mayman, P., Eichhorn, W., Krebs, D., Jhabvala, M., Gezari, D. Y., Fixsen, D. J., Flores, J., Shakoorzadeh, K., Jungo, R., Hakun, C., Workman, L., Karpati, G., Kichak, R., Whitley, R., Mann, S., Tollestrup, E. V., Eisenhardt, P., Stern, D., Gorjian, V., Bhattacharya, B., Carey, S., Nelson, B. O., Glaccum, W. J., Lacy, M., Lowrance, P. J., Laine, S., Reach, W. T., Stauffer, J. A., Surace, J. A., Wilson, G., Wright, E. L., Hoffman, A., Domingo, G., and Cohen, M., "The Infrared Array Camera (IRAC) for the Spitzer Space Telescope," *ApJS* **154**, 10–17 (Sept. 2004).

Downloaded From: https://www.spiedigitallibrary.org/conference-proceedings-of-spie on 2/8/2019
Terms of Use: https://www.spiedigitallibrary.org/terms-of-use

[4] Mighell, K. J., Glaccum, W., and Hoffmann, W., "Improving the photometric precision of IRAC Channel 1," in [*Space Telescopes and Instrumentation 2008: Optical, Infrared, and Millimeter*], *Proceedings of the SPIEE* **7010**, 70102W (July 2008).

[5] Grillmair, C. J., Carey, S. J., Stauffer, J. R., and Ingalls, J. G., "Improving our understanding of the Spitzer Space Telescope's pointing drifts," in [*Space Telescopes and Instrumentation 2014: Optical, Infrared, and Millimeter Wave*], *Proceedings of the SPIEE* **9143**, 914359 (Aug. 2014).

[6] Krick, J. E., Ingalls, J., Carey, S., von Braun, K., Kane, S. R., Ciardi, D., Plavchan, P., Wong, I., and Lowrance, P., "Spitzer IRAC Sparsely Sampled Phase Curve of the Exoplanet Wasp-14B," *ApJ* **824**, 27 (June 2016).

[7] Ballard, S., Charbonneau, D., Deming, D., Knutson, H. A., Christiansen, J. L., Holman, M. J., Fabrycky, D., Seager, S., and A'Hearn, M. F., "A Search for a Sub-Earth-Sized Companion to GJ 436 and a Novel Method to Calibrate Warm Spitzer IRAC Observations," *PASP* **122**, 1341–1352 (Nov. 2010).

[8] Stevenson, K., Harrington, J., Nymeyer, S., Fortney, J. J., Hardy, R. A., Cubillos, P., and Bowman, W. C., "Analysis of HD 149026b Spitzer Data Using a New Intrapixel Technique," in [*AAS/Division for Planetary Sciences Meeting Abstracts #42*], *Bulletin of the American Astronomical Society* **42**, 1062 (Oct. 2010).

[9] Fraine, J. D., Deming, D., Gillon, M., Jehin, E., Demory, B.-O., Benneke, B., Seager, S., Lewis, N. K., Knutson, H., and Désert, J.-M., "Spitzer Transits of the Super-Earth GJ1214b and Implications for its Atmosphere," *ApJ* **765**, 127 (Mar. 2013).

[10] Lewis, N. K., Knutson, H. A., Showman, A. P., Cowan, N. B., Laughlin, G., Burrows, A., Deming, D., Crepp, J. R., Mighell, K. J., Agol, E., Bakos, G. Á., Charbonneau, D., Désert, J.-M., Fischer, D. A., Fortney, J. J., Hartman, J. D., Hinkley, S., Howard, A. W., Johnson, J. A., Kao, M., Langton, J., and Marcy, G. W., "Orbital Phase Variations of the Eccentric Giant Planet HAT-P-2b," *ApJ* **766**, 95 (Apr. 2013).

[11] Deming, D., Knutson, H., Kammer, J., Fulton, B. J., Ingalls, J., Carey, S., Burrows, A., Fortney, J. J., Todorov, K., Agol, E., Cowan, N., Desert, J.-M., Fraine, J., Langton, J., Morley, C., and Showman, A. P., "Spitzer Secondary Eclipses of the Dense, Modestly-irradiated, Giant Exoplanet HAT-P-20b Using Pixel-level Decorrelation," *ApJ* **805**, 132 (June 2015).

[12] Evans, T. M., Aigrain, S., Gibson, N., Barstow, J. K., Amundsen, D. S., Tremblin, P., and Mourier, P., "A uniform analysis of HD 209458b Spitzer/IRAC light curves with Gaussian process models," *MNRAS* **451**, 680–694 (July 2015).

[13] Morello, G., Waldmann, I. P., and Tinetti, G., "Repeatability of Spitzer/IRAC Exoplanetary Eclipses with Independent Component Analysis," *ApJ* **820**, 86 (Apr. 2016).

[14] Ingalls, J. G., Krick, J. E., Carey, S. J., Stauffer, J. R., Lowrance, P. J., Grillmair, C. J., Buzasi, D., Deming, D., Diamond-Lowe, H., Evans, T. M., Morello, G., Stevenson, K. B., Wong, I., Capak, P., Glaccum, W., Laine, S., Surace, J., and Storrie-Lombardi, L., "Repeatability and Accuracy of Exoplanet Eclipse Depths Measured with Post-cryogenic Spitzer," *AJ* **152**, 44 (Aug. 2016).

[15] Charbonneau, D., Brown, T. M., Noyes, R. W., and Gilliland, R. L., "Detection of an Extrasolar Planet Atmosphere," *ApJ* **568**, 377–384 (Mar. 2002).

[16] Spake, J. J., Sing, D. K., Evans, T. M., Oklopčić, A., Bourrier, V., Kreidberg, L., Rackham, B. V., Irwin, J., Ehrenreich, D., Wyttenbach, A., Wakeford, H. R., Zhou, Y., Chubb, K. L., Nikolov, N., Goyal, J. M., Henry, G. W., Williamson, M. H., Blumenthal, S., Anderson, D. R., Hellier, C., Charbonneau, D., Udry, S., and Madhusudhan, N., "Helium in the eroding atmosphere of an exoplanet," *ArXiv e-prints* **1** (May 2018).

[17] Christiansen, J. L., Ballard, S., Charbonneau, D., Madhusudhan, N., Seager, S., Holman, M. J., Wellnitz, D. D., Deming, D., A'Hearn, M. F., and EPOXI Team, "Studying the Atmosphere of the Exoplanet HAT-P-7b Via Secondary Eclipse Measurements with EPOXI, Spitzer, and Kepler," *ApJ* **710**, 97–104 (Feb. 2010).

[18] Knutson, H. A., Charbonneau, D., Cowan, N. B., Fortney, J. J., Showman, A. P., Agol, E., Henry, G. W., Everett, M. E., and Allen, L. E., "Multiwavelength Constraints on the Day-Night Circulation Patterns of HD 189733b," *ApJ* **690**, 822–836 (Jan. 2009).

[19] Kreidberg, L., Bean, J. L., Désert, J.-M., Benneke, B., Deming, D., Stevenson, K. B., Seager, S., Berta-Thompson, Z., Seifahrt, A., and Homeier, D., "Clouds in the atmosphere of the super-Earth exoplanet GJ1214b," *Nature* **505**, 69–72 (Jan. 2014).

Downloaded From: https://www.spiedigitallibrary.org/conference-proceedings-of-spie on 2/8/2019
Terms of Use: https://www.spiedigitallibrary.org/terms-of-use

[20] Sing, D. K., Lecavelier des Etangs, A., Fortney, J. J., Burrows, A. S., Pont, F., Wakeford, H. R., Ballester, G. E., Nikolov, N., Henry, G. W., Aigrain, S., Deming, D., Evans, T. M., Gibson, N. P., Huitson, C. M., Knutson, H., Showman, A. P., Vidal-Madjar, A., Wilson, P. A., Williamson, M. H., and Zahnle, K., "HST hot-Jupiter transmission spectral survey: evidence for aerosols and lack of TiO in the atmosphere of WASP-12b," *MNRAS* **436**, 2956–2973 (Dec. 2013).

[21] Apai, D., Karalidi, T., Marley, M. S., Yang, H., Flateau, D., Metchev, S., Cowan, N. B., Buenzli, E., Burgasser, A. J., Radigan, J., Artigau, E., and Lowrance, P., "Zones, spots, and planetary-scale waves beating in brown dwarf atmospheres," *Science* **357**, 683–687 (Aug. 2017).

[22] Yang, H., Apai, D., Marley, M. S., Karalidi, T., Flateau, D., Showman, A. P., Metchev, S., Buenzli, E., Radigan, J., Artigau, É., Lowrance, P. J., and Burgasser, A. J., "Extrasolar Storms: Pressure-dependent Changes in Light-curve Phase in Brown Dwarfs from Simultaneous HST and Spitzer Observations," *ApJ* **826**, 8 (July 2016).

[23] Metchev, S. A., Heinze, A., Apai, D., Flateau, D., Radigan, J., Burgasser, A., Marley, M. S., Artigau, É., Plavchan, P., and Goldman, B., "Weather on Other Worlds. II. Survey Results: Spots are Ubiquitous on L and T Dwarfs," *ApJ* **799**, 154 (Feb. 2015).

[24] Page, S., [*The Difference: How the Power of Diversity Creates Better Groups, Firms, Schools, and Societies*], Princeton University Press (2007).

Downloaded From: https://www.spiedigitallibrary.org/conference-proceedings-of-spie on 2/8/2019
Terms of Use: https://www.spiedigitallibrary.org/terms-of-use